

ENSEMBLE MEASUREMENT THAT DECOUPLES THE BINDING AFFINITIES
OF IONIC COMPONENTS OF CETRIMONIUM HALIDES

A Thesis

Presented to the Faculty of the Graduate School
of Cornell University

In Partial Fulfillment of the Requirements for the Degree of
Master of Science

by

Heting Pu

August 2020

© 2020 Heting Pu

ABSTRACT

This thesis discusses the binding behaviors of the ionic components of cetrimonium halides, a common family of capping agents [1, 2], on the surface of pseudospherical gold nanoparticles in aqueous environment. Specifically, the reaction kinetics of the adsorption reaction were studied and the behaviors of cetrimonium halide compounds, as well as their cation and anion components, are decoupled and compared.

The binding behaviors of capping agents on gold surfaces were revealed with the assistance of the probe reaction of resazurin reduction. The adsorption reaction kinetics of cetrimonium chloride (CTAC) was proven to be similar to that of isolated CTA^+ . Meanwhile, the binding affinity of chloride anion (Cl^-) towards gold surface is much weaker compared to both CTAC and CTA^+ . These results indicate the dominant effect of CTA^+ in the adsorption behavior of CTAC on amorphous gold surface, and the weak interaction as well as the possible selectivity of Cl^- adsorption on gold facets. These results, although specific to CTAC, is also a part of a general observation over the binding behaviors of the entire family of cetrimonium halides.

Thus, future research has also been planned to study other species in the family of cetrimonium halides, such as cetrimonium bromide (CTAB), and to make effective comparisons between it and Br^- . Such comparisons are worthwhile to discuss, along with the already studied case of CTAC and Cl^- , because halide ion is a component of

the dissolved cetrimonium halides, but also by itself a family of capping agent, with different affinity towards gold surface and different shape directing preferences compared to cetrimonium halides, according to previous research [1, 2]. With experiments that extend to more halide and cetrimonium halide species, we might be able to make a general conclusion and find the reason for the differences between their properties as capping agents for gold nanoparticles.

BIOGRAPHICAL SKETCH

Heting Pu was born on August 18, 1997 in Wuxi, Jiangsu Province, China. She graduated from the international department of Big Bridge Academy, Wuxi in 2015. She earned her Bachelor of Science (B.S.) degree with Department Honor in General Chemistry in 2019 from the University of California, Los Angeles. In the undergraduate years, she researched on the metal nanomaterials under the mentorship of Prof. Xiangfeng Duan. She worked on the shape-controlled synthesis of platinum-based nanomaterials, specifically on the development of the synthetic methods of PtNi tetrahedral nanoparticles and Pt-based alloy nanowires with core-shell structure. She also worked on the improvement of the catalytic ability of these produced materials on fuel cell reactions such as oxygen reduction reaction and hydrogen evolution reaction.

After college, she entered Cornell University in Ithaca, NY to pursue her Master of Science (M. S.) degree in Chemistry under the supervision of Prof. Peng Chen. Her work focused on the analysis of the reaction dynamics of nonfluorescent reactions on the gold surface, visualized with the probe reaction of resazurin reduction. For her master thesis, she worked on the topic of the decoupled ionic adsorption behavior of ionic compounds. She plans to continue the research on precious metal nanomaterials and their catalytic application in the future pursuit of Ph.D. degree.

ACKNOWLEDGMENTS

The one year I spent in the master program of Cornell University is short, still, I have met many people that have generously provided help and instructions to my study and research. I would like to extend my most gratitude to Prof. Peng Chen for his supervision over my research in this year. The communication with Prof. Chen has greatly improved my skills in independent research as well as critical thinking. He has instructed my research and provided numerous advises on my experiment, data process and thesis writing.

I would also like to thank Dr. Rocky Ye, for the hands-on help with my operation of experiment equipment, chemical purchase, the providing of some basic MATLAB codes for data process, and most importantly, the instruction on the theoretical calculation with Langmuir-Hinshelwood Kinetics. All members in Chen lab are so supportive, and I do want to thank every one of them for even the most trivial help in my daily experiment.

TABLE OF CONTENTS

ABSTRACT.....	ii
BIBLIOGRAPHICAL SKETCH.....	iv
ACKNOWLEDGEMENTS.....	v
LIST OF FIGURES.....	viii
LIST OF TABLES.....	x
1. INTRODUCTION.....	11
2. EXPERIMENTS AND RESULTS.....	14
2.1. The Use of Resazurin as the Probe of the Reaction.....	14
2.2. Langmuir-Hinshelwood Kinetics.....	15
2.3. The Adsorption Equilibrium Constant of Resazurin and Capping Agents.....	16
3. DISCUSSION.....	21
3.1. The Decoupled Binding Affinities of Ions.....	21
3.2. Expected Future Works.....	24
3.2.1. Future Experiments on Br ⁻	24
3.2.2. Facet-specific Experiments.....	25

3.2.3. Concurrent Ionic Interactions with Adsorption Activities.....	26
4. MATERIALS AND METHODS.....	27
4.1. Materials.....	27
4.2. Experimental Procedures.....	27
APPENDIX-ADDITIONAL DATA.....	29
REFERENCES.....	32

LIST OF FIGURES

Figure 1 A) The structure of cetrimonium bromide (CTAB) and cetrimonium chloride (CTAC). **B)** The surface adsorption behavior of CTAB on the surface of gold nanoparticle, modeled with molecular dynamic simulations technique [13]. The yellow spheres represent gold atoms, the blue lines represent the organic backbones of CTA⁺ cations with the blue spheres as nitrogen atom.

Figure 2 A) The structures of resazurin and resorufin. **B)** The absorption spectrum monitored over the progress of the Rz reduction reaction, within the wavelength window from 500nm to 700nm. The initial concentration $[Rz]_0$ was 13.72 μ M. As the reaction progresses, the Rz absorption peak at 605nm gradually diminishes, and the Rf absorption peak at 574nm rises.

Figure 3 A) The monitored concentration change of Rz with $[Rz]_0$ of 13.72 μ M, as an example. The absorption spectra were scanned for every 2 minutes. All the concentration data were calculated from Rz absorption at 605nm and Beer-Lambert Law. The reaction rate was approximated with 1st order reaction mechanism with respect to Rz. **B)** The initial rates of Rz reduction reaction at different $[Rz]_0$, fitted to Eqn. 1 of L-H model to obtain the values of k and K_{Rz} .

Figure 4 The initial reaction rate at different initial concentrations of **A)** CTAB; **B)** CTAC; **C)** CTAOH and **D)** KCl, all fitted to the L-H model with two competitive

adsorption species (Eqn. 2). The values K in each plot denote the adsorption equilibrium constant of each capping agent.

Figure 5 The listed adsorption equilibrium constants of CTAB, CTAC, CTAOH and KCl, along with their range of uncertainty, calculated from Eqn. 2 of L-H model.

Figure 6 The monitored concentration change of Rz with various $[Rz]_0$. The reaction rates were approximated with 1st order reaction mechanism with respect to Rz.

Figure 7 The monitored concentration change of Rz with $[Rz]_0$ of 13.72 μ M, at the presence of CTAC. The reaction rates were approximated with 1st order reaction mechanism with respect to Rz.

Figure 8 The monitored concentration change of Rz with $[Rz]_0$ of 13.72 μ M, at the presence of CTAC. The reaction rates were approximated with 1st order reaction mechanism with respect to Rz.

Figure 9 The monitored concentration change of Rz with $[Rz]_0$ of 13.72 μ M, at the presence of CTAOH. The reaction rates were approximated with 1st order reaction mechanism with respect to Rz.

Figure 10 The monitored concentration change of Rz with $[Rz]_0$ of 13.72 μ M, at the presence of KCl. The reaction rates were approximated with 1st order reaction mechanism with respect to Rz.

LIST OF TABLES

Table 1 The adsorption equilibrium constants corresponding to each of the capping agent tested, calculated with the obtained K_{Rz} value and the L-H model.

Table 2 The species that chemically adsorbs on the surface of gold, upon the introduction of capping agents to the aqueous gold nanoparticle solution.

1. INTRODUCTION

The development of noble metal nanoparticles has been an extensively studied topic for decades due to their use in numerous fields of industry and research [3, 4, 5]. Among them, gold nanoparticles have received special attention because of their wide applications in catalysis, photovoltaics, biomedicine, sensory probes and many other fields [6, 7, 8]. The wide use of gold nanoparticles has also spurred the development of numerous well-verified synthetic methods of shape-controlled gold nanostructures [9, 10]. A systematic synthetic procedure leading to gold nanoparticles in pseudospherical shapes was developed in as early as 1951 by Turkevich et. al. [11]. In the subsequent decades, derivatives of the Turkevich method have continued to further produce gold nanoparticles with different shapes and surface morphologies [1].

Nowadays, methods are well developed for synthesis of gold nanoparticles with controllable shapes [9]. This kind of control is achieved by the surface adsorption of capping agents on gold surfaces. Capping agents are chemical species that can adsorb to surface atoms and form adsorption complexes. In the process of gold nanoparticle synthesis, the formation of adsorption complexes between capping agent molecules and surface gold atoms would block the further deposition of gold onto these adsorbed sites, and thus affect the growth of the nanoparticles. Some capping agents prefer to adsorb on some specific gold facets, which lead to the growth of the particle along other less affected facets, and eventually affect the final shape and size of the nanoparticles [12, 13, 14].

In synthetic procedures, one specific kind of capping agent, cetrimonium halide ($C_{19}H_{42}NX$, Figure 1), is frequently used as a primary size-confining and shape-directing agent [2, 10]. At the same time, halide ions by themselves are also a group of commonly used shape-controlling agents and have been proposed to have significant effect on the facet selectivity of the growth of gold nanoparticles [14]. Although cetrimonium halide salts ionize in aqueous solution and thereby produce halide ions in addition to CTA^+ ion, the shape directing preference of cetrimonium halides was not consistent with that of individual halide anions as revealed by previous research. Here we propose that this difference is caused by the presence of cetrimonium cation, $C_{19}H_{42}N^+$ (CTA^+).

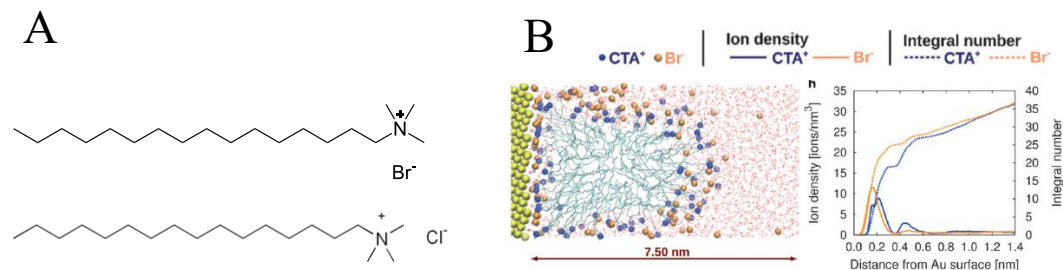


Figure 1 **A)** The structure of cetrimonium bromide (CTAB) and cetrimonium chloride (CTAC). **B)** The surface adsorption behavior of CTAB on the surface of gold nanoparticle, modeled with molecular dynamics simulations technique [12]. The yellow spheres represent gold atoms, the blue lines represent the organic backbones of CTA^+ cations with the blue spheres as nitrogen atom.

It is important to understand the different behaviors of the CTA^+ and halide ions in the same system, as cetrimonium halides are dissolved and do not function as a whole compound in real life experimental systems. Papers discussing the interactions

between cetrimonium halides and gold had mostly approached this topic by visualizing the distribution density of CTA^+ and halide anions within short distances from gold surfaces, using methods such as quantitative imaging and spectroscopies [13] or theoretical modeling techniques like molecular dynamics simulations [12, 20] (Figure 1). However, these results only showed the presence of capping ligands around gold nanoparticles, which may as well be caused by various molecular behaviors such as Van der Waals interactions and the electrostatic requirement that charges are nearly balanced in any reasonable volume. These techniques are largely incapable of demonstrating whether any of these ions are actually connected to the gold surface via adsorption. Furthermore, both CTA^+ and halide ions are present in the measurements or simulations of these research, thus they failed to decouple the individual adsorption activities of the CTA^+ and halide anions.

In this work we use an ensemble titration system and UV-vis spectrometry to study both combined and decoupled adsorption activities of CTA^+ and halide ions on the amorphous surface of pseudospherical gold nanoparticles (the readily available gold nanomaterials in the Chen lab). With the help of a probe reaction catalyzed by gold atoms, we were able to reveal the actual binding preferences of CTA^+ and halide ions on gold surface active sites, and exclude the effect of other molecular behaviors that would also bring capping agents close to the gold nanoparticles. In the following sections, the binding affinities of CTA^+ , halide anions and cetrimonium halide compounds are measured and compared.

2. EXPERIMENTS AND RESULTS

2.1. The Use of Resazurin as the Probe of the Reaction

Resazurin (Rz, 7-Hydroxy-3*H*-phenoxazin-3-one 10-oxide) is commonly used as a dye or probe in general catalytic and biological experiments [15], because of its intense color and strong absorption of visible light at wavelength of around 605nm. Rz is redox sensitive and can be irreversibly reduced to resorufin (Rf, 7-Hydroxy-3*H*-phenoxazin-3-one) [16], a compound with pink-purple color which has a primary absorption peak around 574nm (Figure 2).

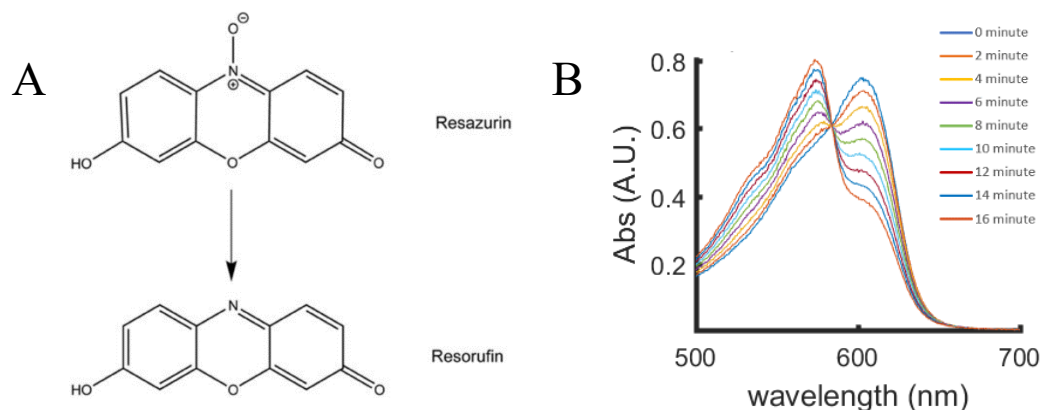


Figure 2 **A)** The structures of resazurin and resorufin [22]. **B)** The absorption spectrum monitored over the progress of Rz reduction reaction, within the wavelength window from 500nm to 700nm. The initial concentration $[Rz]_0$ was $13.72\mu\text{M}$. As the reaction progresses, the Rz absorption peak at 605nm gradually diminishes, and the Rf absorption peak at 574nm rises.

In this experiment, the reduction reaction from Rz to Rf by NH_2OH was catalyzed on the surface of pseudospherical gold nanoparticles. With the presence of capping agents such as cetrimonium halide, their chemical adsorption with surface gold atoms would reduce the amount of gold available to catalyze Rz reduction, and as a result slow down the rate of the reaction. It is also true the other way around, that the reaction rate of Rz reduction would reflect the surface adsorption condition of capping agents, and this relation can be numerically represented and calculated with the application of surface adsorption models, such as the Langmuir-Hinshelwood Kinetics.

Before the conduction of the ensemble titration measurement, the UV-Vis spectrometry of Rz was first checked. The optimal concentration of Rz for the reaction had to be experimentally determined. The Rz used in this project had been manually recrystallized to higher purity from the as-purchased product, and as a result, the accurate concentration of it was unknown in the first place. The concentration of Rz used throughout this experiment was obtained by a 500-fold dilution from the stock solution, and was determined to be $13.72\mu\text{M}$ using Beer-Lambert Law, with absorption of 0.75 at 605nm. The absorption value is recommended to be smaller than 1 so that it fits to the ideal condition of Beer-Lambert Law with good correspondence. At the same time, the initial absorption value should still be large enough, so that later on, absorption at 605nm was still detectable after most Rz had been consumed along the reaction progress. The absorption value of 0.75 fell within these two requirements, and a 500-fold dilution was easily operable and accurately repeatable in experiments.

2.2. Langmuir-Hinshelwood Kinetics

For most of the reactions facilitated by catalysts, the rates of the reactions are often significantly affected by the kinetics of the catalysis step. Langmuir-Hinshelwood (L-H) Kinetics is a commonly applied model in the discussion of heterogeneous catalytic systems [17]. It connects the reaction rate v and the rate constant k of the reaction that is catalyzed, with the kinetics of the adsorption activity between the reagent and the catalyst, specifically with the equilibrium constant K of the substrate adsorption activity on the catalyst [18]. For the reduction of Rz on the surface of gold nanoparticles in aqueous solution, without the presence of any capping agent, the kinetics is expressed as:

$$v_{Rz} = \frac{k_{Rz} \cdot K_{Rz} \cdot [Rz]}{1 + K_{Rz} \cdot [Rz]} \quad \text{Equation 1}$$

In Eqn. 1, the v_{Rz} and $[Rz]$ terms correspond to the initial reaction rate of Rz reduction and the initial Rz concentration. In the experiment, they were directly obtained from the UV-vis data. k_{Rz} is the rate constant of Rz reduction, and K_{Rz} is the adsorption equilibrium constant between Rz and gold atoms under the experimental conditions. These two parameters were calculated by data fitting using v_{Rz} , $[Rz]$ and Eqn. 1.

With the addition of a capping agent into the reaction environment, the system would then follow the model of L-H kinetics with two adsorbents. Here we assume

that the kinetics of each of the adsorption activities of these two adsorbents are not affected by the presence of each other, and the rate of the reaction is then expressed as:

$$v_{RZ} = \frac{k_{RZ} \cdot K_{RZ} \cdot [RZ]}{1 + K_{RZ} \cdot [RZ] + K_{CA} \cdot [CA]} \quad \text{Equation 2}$$

where [CA] corresponds to the initial concentration of the capping agent, and K_{CA} is the adsorption equilibrium constant of the capping agent present in the system. In this work, Eqn. 2 applies to all the capping agents studied, including the cetrimonium salts and the cation and anions. With each of the other parameters known from experimental set-up and previous calculation, the value of K_{CA} can be determined by data fitting.

Many reasons would cause the capping agents to be present near to gold surface, such as adsorption reaction, local balance of charges, or even the simple free motion of molecules. Methods used in previous research, including imaging [14], were unable to tell whether the molecules they saw were chemically adsorbed to gold surface or are simply there without any actual contact with gold. The value of K_{CA} obtained from L-H Kinetics is specific to the adsorption activity, and thus distinguishes the portion of the capping agents that chemisorb on gold from all other capping agents simply present close to the gold surface, which would not slow down the probe reaction and thus would not be detected.

A large K_{CA} value indicates that the adsorption reaction prefers the formation of the chemisorbed complex, and suggests a strong binding affinity of adsorbent on the surface of gold nanoparticle. In contrast, a small K_{CA} value indicates weak binding

activity towards the gold surface, with the information that the adsorption reaction prefers not to occur.

2.3. The Adsorption Equilibrium Constant of Resazurin and Capping Agents

First of all, the value of K_{Rz} was calculated by titrating the Rz reduction reaction with different $[Rz]_0$ ranging from zero to 15 micromolar. The reaction rate was approximated with the 1st order mechanism with respect to the consumption of Rz. The different rates of the reaction with respect to different $[Rz]_0$ were fitted into Eqn. 1, and the k_{Rz} and K_{Rz} values were then calculated (Figure 3). The obtained value of k_{Rz} is 767.53 ± 74.99 nM/min, and the calculated K_{Rz} value is 0.18 ± 0.05 μM^{-1} .

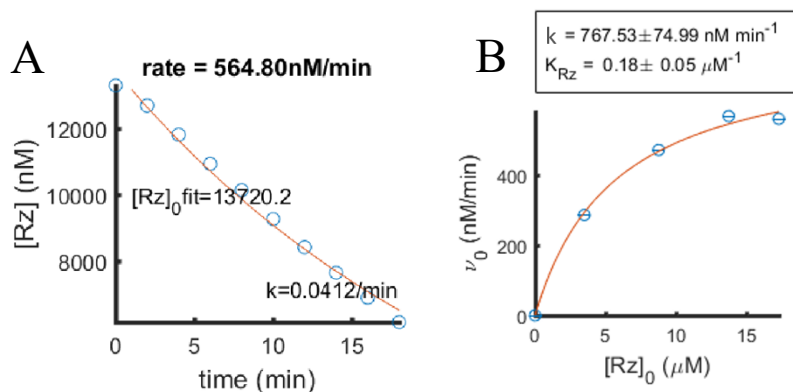


Figure 3 **A)** The monitored concentration change of Rz with $[Rz]_0$ of $13.72 \mu\text{M}$, as an example. The absorption spectra were scanned for every 2 minutes. All the concentration data were calculated from Rz absorption at 605nm and Beer-Lambert Law. The reaction rate was approximated with 1st order reaction mechanism with respect to Rz. **B)** The initial rates of Rz reduction reaction at different $[Rz]_0$, fitted to Eqn. 1 of L-H model to obtain the values of k and K_{Rz} .

The different capping agents were then tested. Among all the common halide and cetrimonium halide capping agents planned to be experimented on, the test of CTAB, CTAC, CTAOH and KCl were possible to carry out. For every one of these four capping agents, a series of Rz reduction reactions were performed with the concentration of Rz fixed at 13.72 μ M, and with other reaction parameters kept as constants as well. The set up of the reaction was almost the same as the previous test of k_{Rz} and K_{Rz} , and the only difference is the addition of a capping agent. The only variable in each series of reactions is the different concentrations of the designated capping agent, which caused the different rates of Rz reductions within each series. Thus, each of the capping agent was then associated with a set of reaction rates corresponding to a set of concentrations.

The values of rate constant k_{RzS} and adsorption equilibrium constant K_{CAS} (Table 1) were then calculated for each of the four capping agents, by fitting the four series of reaction rates to Eqn. 2 of L-H model, along with the previously calculated K_{Rz} and k_{Rz} (Figure 4).

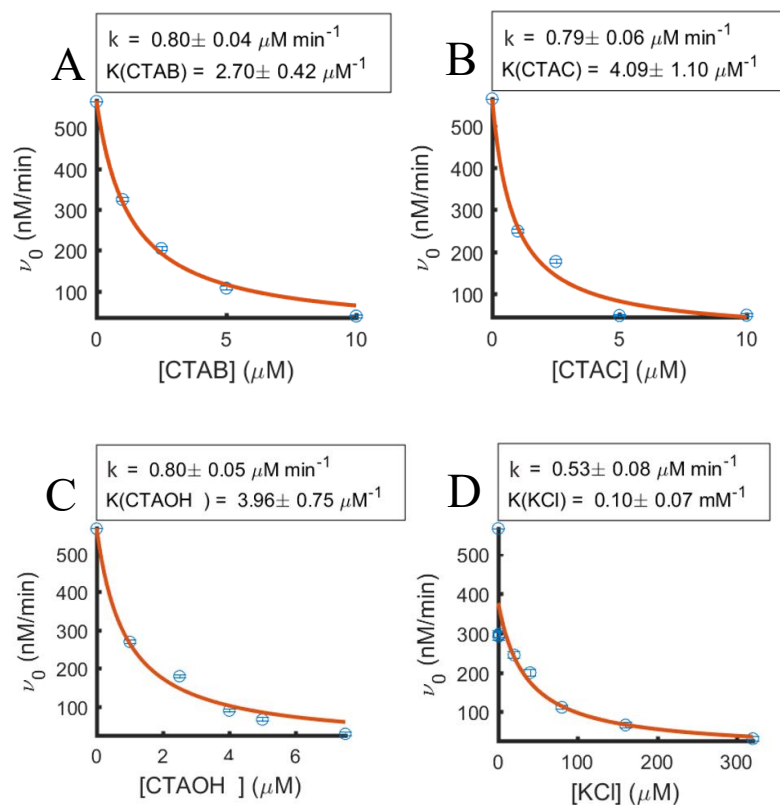


Figure 4 The initial reaction rate at different initial concentrations of **A)** CTAB; **B)** CTAC; **C)** CTAOH and **D)** KCl, all fitted to the L-H model with two competitive adsorption species (Eqn. 2). The values K in each plot denote the adsorption equilibrium constant of each capping agent.

Capping Agent	Adsorption Equilibrium Constant K
CTAB	$2.70 \pm 0.42 \mu\text{M}^{-1}$
CTAC	$4.09 \pm 1.10 \mu\text{M}^{-1}$
CTAOH	$3.96 \pm 0.75 \mu\text{M}^{-1}$
KCl	$0.10 \pm 0.07 \text{mM}^{-1}$

Table 1 The adsorption equilibrium constants corresponding to each of the capping agent tested, calculated with the obtained K_{RZ} value and the L-H model.

3. DISCUSSION

3.1. The Decoupled Binding Affinities of Ions

The local charges at close vicinity to the gold surface may be balanced by the presence of ions with opposite charges to the capping agent species, such as OH^- and K^+ , but they do not behave the same as capping agents. Since the hydroxide anion does not adsorb on gold surface in this reaction system, the adsorption equilibrium constant of CTAOH contains the contribution from CTA^+ only, thus K_{CTAOH} can be as well denoted as K_{CTA^+} . Similarly, since the compound KCl dissolves completely in aqueous solution, the value of K_{KCl} could be viewed as equivalent to K_{Cl^-} , considering that no significant potassium adsorption activity has been reported in the synthesis of gold nanostructure, indicating that K^+ cation would not be present on gold surface with notable density in this experiment. Thus, the adsorption equilibrium constants measured from CTAOH and KCl reflect the individual binding affinities of CTA^+ ion and Cl^- ion.

By applying L-H model to CTAB and CTAC, the Eqn. 2 considered the integrated effect of both cation and anion species on the rate of the probe reaction. As a result, K_{CTAC} and K_{CTAB} describe the altogether adsorption behavior of both CTA^+ and corresponding halide ions.

Capping Agent	Adsorbed Species on Gold Surface
CTAB	CTA ⁺ , Br ⁻
CTAC	CTA ⁺ , Cl ⁻
CTAOH	CTA ⁺
KCl	Cl ⁻

Table 2 The species that chemically adsorbs on the surface of gold, upon the introduction of capping agents to the aqueous gold nanoparticle solution.

The adsorption equilibrium constants of CTAC, CTAB and CTAOH are in the same order of magnitude. The values can be viewed as comparable and similar within the range of error. Specifically, the value of K_{CTAOH} completely overlaps within the range of error of K_{CTAC} , and they can be considered as experimentally highly similar. In contrast, the value of K_{Cl^-} is significantly smaller than the equilibrium constant of cetrimonium-containing species (Figure 5). It is four orders of magnitude smaller than all of the K_{CTAC} , K_{CTAB} and K_{CTA^+} , and has no overlap with them even considering the range of errors.

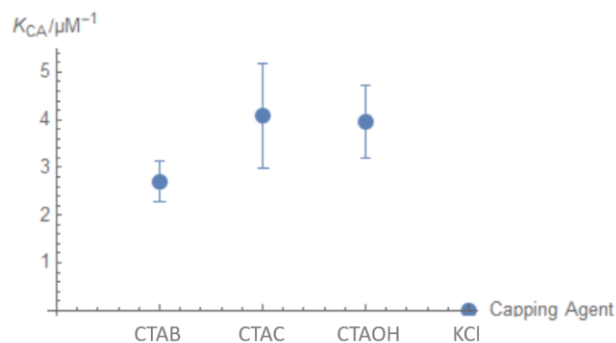


Figure 5 The listed adsorption equilibrium constants of CTAB, CTAC, CTAOH and KCl, along with their range of uncertainty, calculated from Eqn. 2 of L-H model.

The small value of K_{Cl^-} suggests that the Cl^- anion adsorbs weakly on the amorphous surface of pseudospherical gold nanoparticles. Under the chemical environment of this experiment and compared to cetrimonium species, Cl^- anion much more prefers freely dissolved status rather than the formation of adsorption complex with gold. Comparing the value of K_{Cl^-} , K_{CTA^+} and K_{CTAC} , we clearly see that K_{CTA^+} is significantly more similar to K_{CTAC} than K_{Cl^-} . Thus, we are able to conclude that the binding affinity of CTA^+ cation is much higher than Cl^- anion on amorphous gold surface in aqueous solution. The contribution of Cl^- anion to the binding affinity of CTAC is negligible compared to the contribution of CTA^+ cation. The obtained result suggests that the CTA^+ cation is the major contributor to the reported size-confining ability of CTAC during the synthesis of gold nanostructure.

The surface of pseudospherical gold nanoparticle is composed of a mix of various high and low index facets. High binding affinity towards the surface of pseudospherical particles suggests that the CTA^+ cation is generally not significantly selective to the sites and facets that it binds to, and actively binds to most, or maybe all of the available binding sites. On the other hand, the low adsorption affinity of Cl^- ion indicates that although it certainly binds to the surface of gold, which is supported by previous research, it is possible that Cl^- ion binds to active sites selectively. It might have a preference of one or a few specific facets that it adsorbs to, and might have low affinities towards other facets, which results in the low general binding affinity on the surface of pseudospherical nanoparticles, as well as its shape-directing ability in the synthesis of gold nanoparticles. However, these suggestions require further experiments to get confirmed in detail.

3.2. Expected Future Works

With the accomplished experiments, the binding affinities of CTA^+ and Cl^- were measured separately and compared to the affinity of CTAC. This successfully draws the conclusion that the CTA^+ plays a much more significant role in the binding activities of CTAC compared to Cl^- .

3.2.1 Future Experiments on Br^-

While the data of CTAB was also obtained, there was not enough time to experiment on KBr (although the experiment had been planned) and to decouple the ionic components of CTAB. The value of K_{CTAB} is $2.70 \pm 0.42 \mu\text{M}^{-1}$, which is of the same order of magnitude compared to K_{CTAC} and K_{CTA^+} , but at the same time, it is also notably smaller than the other two. The reason for this difference remains unknown unless more repeated experiments were performed to reduce the error and to improve the accuracy of the data, as well as unless additional experiments were carried out on Br^- , CTA^+ and CTAB to reveal the possible impact of Br^- on the binding behavior of CTA^+ , that was not observed on Cl^- .

As reported in previous research, the binding energies of Br^- (the energy required to put in to dissociate a adsorption complex) on various gold facets are generally smaller compared to the binding energies of Cl^- [19]. This observation indicates that the Au-Br chemisorbed complex is less stable compared to the Au-Cl

complex. According to this information, we may hypothesize that the expected K_{Br^-} tested with our experiment method would be smaller than K_{Cl^-} . This hypothesis, same as the observed smaller K_{CTAC} value discussed in previous paragraph, could only be verified and explained by future experiments. With this expected data of CTAB, CTAC, Br^- and Cl^- , we would be able to conclude whether or not a general relation exists between the halide and the cetrimonium halide species.

3.2.2 Facet-specific Experiments

With the obtained data, it is already confirmed that the cation and anion components of cetrimonium halides behave differently in the surface adsorption activity on amorphous gold surface. Question remains, that the adsorption activities of these ions corresponding to specific facets remain unknown. This is a question that worth to ask since the synthesis of gold nanostructures in recent years has been increasingly focused on the selectivity of the growth of facets [1]. The same experiment could be repeated on gold nanocube (surrounded by [100] facets), nanotetrahedron or octahedron (surrounded by [111] facets), as well as on bipyramid or rhombic dodecahedron (surrounded by [110] facets), as long as we could find some probe reactions that these facets are able to catalyze with measurable rates. These particles with specific shapes are generally not commercialized and require extra lab time and materials to synthesize.

3.2.3 Concurrent Ionic Interactions with Adsorption Activities

Although the cetrimonium halide species dissolve completely in aqueous reaction environments, weak interactions may still exist between the charged cations and anions. It has been reported that the distribution densities of CTA^+ and Br^- are similar near the surface of the gold, which might be caused by the balance of local charges, although it is proven in the previous sections that the amounts of the CTA^+ and halide ions chemisorbed on the gold surface are different [12, 20]. It is worthwhile to ask that whether or not the ionic interactions between capping agents would affect the binding behaviors of them, because ionic interactions might change the energy of the ions, and might stabilize their behaviors. If such interactions do change the binding kinetics of individual ions, we would also want to measure to what extent are the binding behaviors affected.

The direct comparisons between K_{CTAC} and K_{CTA^+} , as well as between K_{CTAC} and K_{Cl^-} in previous sections are made under the approximation that in the measurement of CTAC, the individual binding affinities of CTA^+ and Cl^- are not affected by the ionic interaction with each other when they are both present. If such ionic interactions do affect the integrated binding behaviors of CTAC, some correcting factors would be required in these data analyses. The existence of such interaction between different adsorbents may be tested and measured by comparing the behaviors of capping agents with models of adsorption cooperativity, such as the Hill equation [21], or by monitoring whether the binding affinity of a capping agent is changed with the presence of an oppositely-charged ionic species that is not an adsorbent.

4. MATERIALS AND METHODS

4.1. Materials

The pseudospherical gold nanoparticles used in the experiment (Ted Pella 15702-20) are generally around 5nm in diameter, with uniform shape and sizes, and are stored under refrigeration. The gold particles were monodispersed in water, along with trace amount of citrate, tannic acid and potassium carbonate that were inherently contained in the as-purchased product. CTAB (>99%), CTAC (>98%), CTAOH (10% wt in H₂O) and NH₂OH (99%) were purchased from Sigma-Aldrich. Self-purified resazurin was used, and its accurate concentration was determined with UV-Vis spectrometry and Beer-Lambert law. The reactions were carried out in 100mM phosphate buffer. During the progress of UV-vis spectrometry, reusable quartz cuvette with path length of 1cm was used. All the spectrometry data were analyzed and fitted to L-H model via MATLAB codes.

4.2. Experimental Procedures

In a UV-vis cuvette, phosphate buffer was first added with corresponding amount that made sure the final volume of the reaction solution was always 2mL. Then, 2 μ L of 1M NH₂OH aqueous solution, 4 μ L of Rz aqueous solution and various

volume of capping agent solution were added into the cuvette sequentially. Finally, 240 μ L of gold nanoparticle solution was injected to initiate the reduction of Rz, and the cuvette was then immediately capped. After vigorously shaking for 1 to 2 seconds, the cuvette was quickly put into the spectrometry and scanned with UV-vis spectrometry over the range of wavelength from 500 to 700nm.

Over the progress of Rz reduction reaction, the spectrometry of the reaction solution was scanned for every 2 minutes for reactions with Rz only. For reactions with the presence of CTAC, CTAB and CTAOH, the absorption spectra were collected for every 5 minutes due to the slow reaction speed. The interval between scans for the reactions with the presence of KBr was 1 minute. A total of 10 scans were taken for each reaction, and a series of reactions with different concentrations of capping agents were carried out for the calculation of adsorption equilibrium constant.

APPENDIX-ADDITIONAL DATA

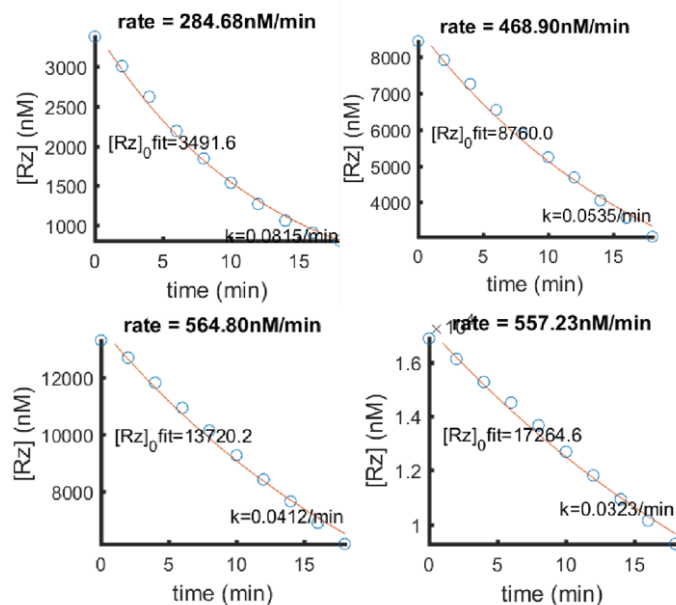


Figure 6 The monitored concentration change of Rz with various $[Rz]_0$. The reaction rates were approximated with 1st order reaction mechanism with respect to Rz.

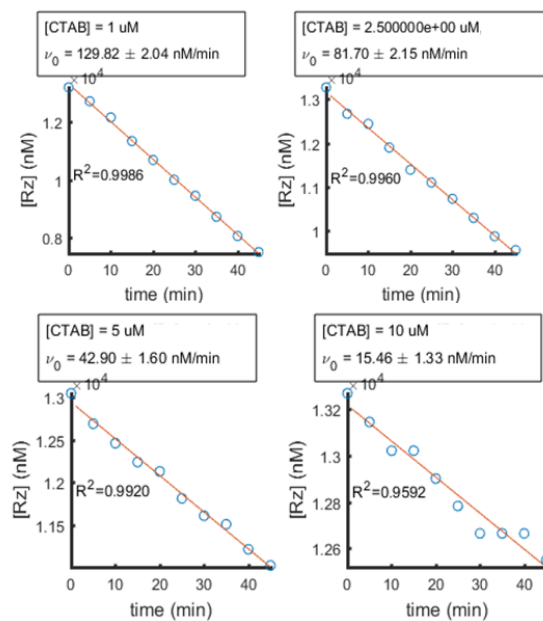


Figure 7 The monitored concentration change of Rz with $[Rz]_0$ of $13.72\mu\text{M}$, at the presence of CTAC. The reaction rates were approximated with 1st order reaction mechanism with respect to Rz.

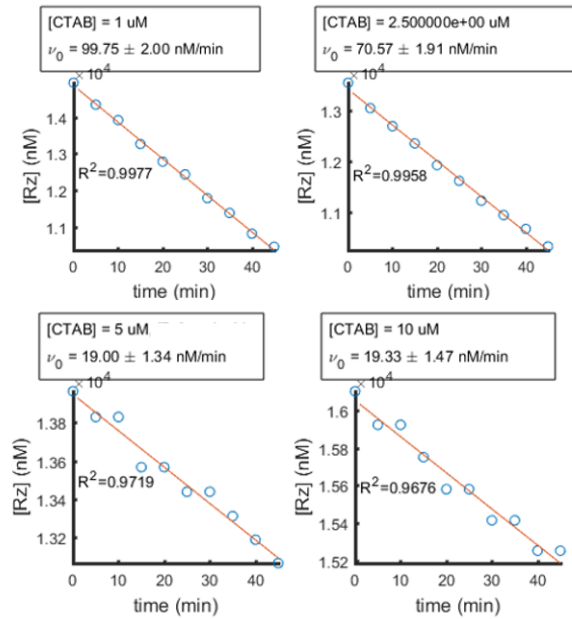


Figure 8 The monitored concentration change of Rz with $[Rz]_0$ of $13.72\mu\text{M}$, at the presence of CTAC. The reaction rates were approximated with 1st order reaction mechanism with respect to Rz.

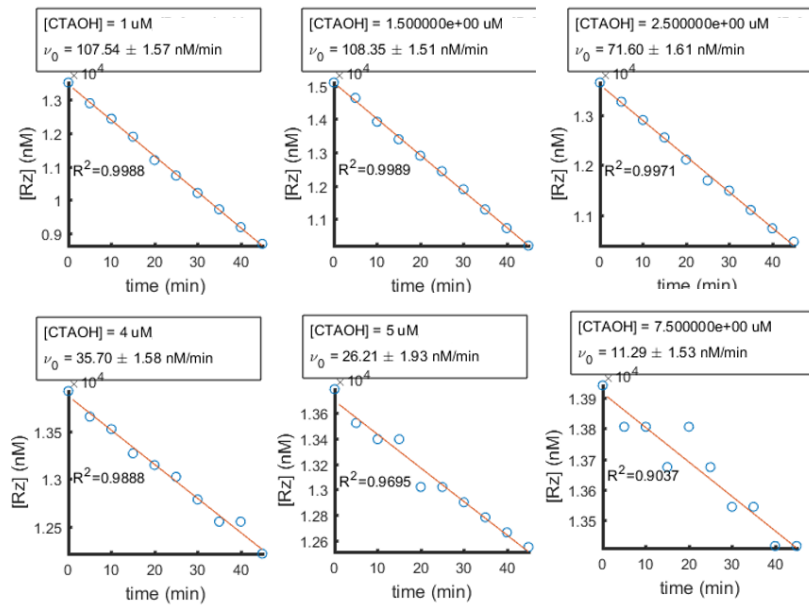


Figure 9 The monitored concentration change of Rz with $[Rz]_0$ of $13.72\mu\text{M}$, at the presence of CTAOH. The reaction rates were approximated with 1st order reaction mechanism with respect to Rz.

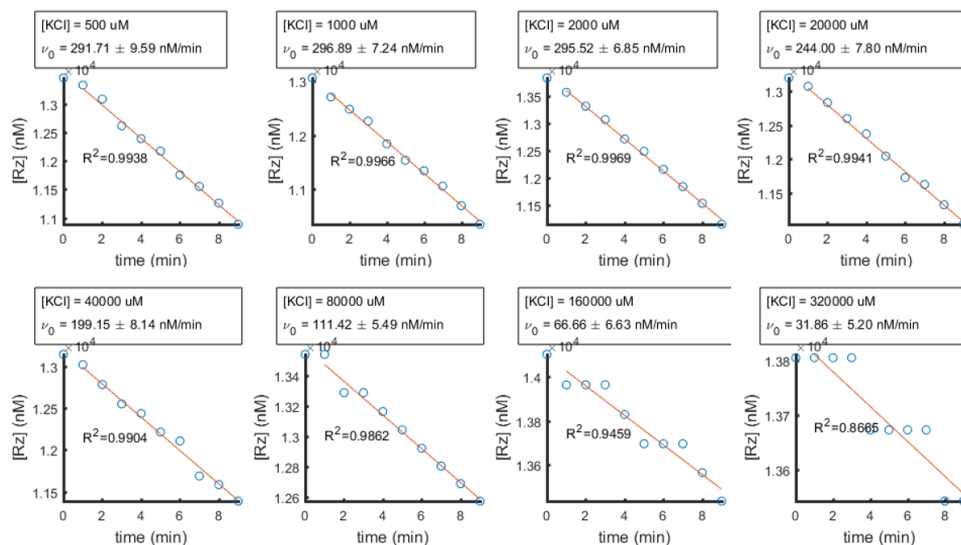


Figure 10 The monitored concentration change of Rz with $[\text{Rz}]_0$ of $13.72\mu\text{M}$, at the presence of KCl. The reaction rates were approximated with 1st order reaction mechanism with respect to Rz.

REFERENCES

- [1] M. Grzelczak, J. Pérez-Juste, P. Mulvaney and L. M. Liz-Marzán, "Shape control in gold nanoparticle synthesis," *Chemical Society Reviews*, vol. 37, no. 9, pp. 1783-1791, 2008.
- [2] R. Becker, B. Liedberg and P.-O. Käll, "CTAB promoted synthesis of Au nanorods – Temperature effects and stability considerations," *Journal of Colloid and Interface Science*, vol. 343, no. 1, pp. 25-30, 2010.
- [3] S. Guo and E. Wang, "Noble metal nanomaterials: Controllable synthesis and application in fuel cells and analytical sensors," *Nanotoday*, vol. 6, no. 3, pp. 240-264, 2011.
- [4] G. Gangadhar, U. Maheshwari and S. Gupta, "Application of Nanomaterials for the Removal of Pollutants from Effluent Streams," *Nanoscience & Nanotechnology-Asia*, vol. 2, no. 2, pp. 140-150, 2012.
- [5] Y. Cao, J. Zhang, Y. Yang, Z. Huang, N. V. Long and C. Fu, "Engineering of SERS Substrates Based on Noble Metal Nanomaterials for Chemical and Biomedical Applications," *Applied Spectroscopy Reviews*, vol. 50, no. 6, pp. 499-525, 2015.
- [6] Y. Jv, B. Li and R. Cao, "Positively-charged gold nanoparticles as peroxidase mimic and their application in hydrogen peroxide and glucose detection," *Chemical Communications*, no. 42, pp. 8017-8019, 2010.
- [7] H. Daraee, A. Eatemadi, E. Abbasi, S. F. Aval, M. Kouhi and A. Akbarzadeh, "Application of gold nanoparticles in biomedical and drug delivery," *Artificial Cells, Nanomedicine, and Biotechnology*, vol. 44, no. 1, pp. 410-422, 2016.
- [8] Z. H. Chen, Y. B. Tang, C. P. Liu, Y. H. Leung, G. D. Yuan, L. M. Chen, Y. Q. Wang, I. Bello, J. A. Zapien, W. J. Zhang, C. S. Lee and S. T. Lee, "Vertically Aligned ZnO Nanorod Arrays Sentsized with Gold Nanoparticles for Schottky Barrier Photovoltaic Cells," *J. Phys. Chem.*, vol. 113, no. 30, p. 13433–13437, 2009.
- [9] J. Xiao and L. Qi, "Surfactant-assisted, shape-controlled synthesis of gold nanocrystals," *Nanoscale*, no. 4, pp. 1383-1396, 2011.
- [10] Y. Sun and Y. Xia, "Shape-Controlled Synthesis of Gold and Silver Nanoparticles," *Science*, vol. 298, no. 5601, pp. 2176-2179, 2002.
- [11] J. Turkevich, P. Stevenson and J. Hillier, "A study of the nucleation and growth processes in the synthesis of colloidal gold," *Discuss. Faraday Soc.*, vol. 11, pp. 55-75, 1951.
- [12] S. K. Meena and M. Sulpizi, "From Gold Nanoseeds to Nanorods: The Microscopic Origin of the Anisotropic Growth," *Angew. Chem.*, no. 128, p. 12139 –12143, 2016.
- [13] B. E. Janicek, J. G. Hinman, J. J. Hinman, S. Bae, M. Wu, J. Turner, H. Chang, E. Park, R. Lawless, K. S. Suslick, C. J. Murphy and P. Y. Huang, "Quantitative Imaging of Organic Ligand Density on Anisotropic Inorganic Nanocrystals," *Nano Lett.*, no. 19, p. 6308–6314, 2019.

- [14] M. Kasture, M. Sastry and B. Prasad, "Halide ion controlled shape dependent gold nanoparticle synthesis with tryptophan as reducing agent: Enhanced fluorescent properties and white light emission," *Chemical Physics Letters*, vol. 484, no. 4-6, pp. 271-275, 2010.
- [15] S. Anoopkumar-Dukie, J. B. Carey, T. Conere, E. O'Sullivan, F. N. v. Pelt and A. Allshire, "Resazurin assay of radiation response in cultured cells," *The British Journal of Radiology*, vol. 78, no. 934, pp. 945-947, 2005.
- [16] R. S. Twigg, "Oxidation-reduction aspects of resazurin," *Nature*, vol. 155, no. 3935, pp. 401-402, 1945.
- [17] R. J. Baxter and P. Hu, "Insight into why the Langmuir–Hinshelwood mechanism is generally preferred," *J. Chem. Phys.*, vol. 116, no. 11, pp. 4379-4381, 2002.
- [18] K. V. Kumar, K. Porkodi and F. Rocha, "Langmuir–Hinshelwood kinetics – A theoretical study," *Catalysis Communications*, vol. 9, no. 1, pp. 82-84, 2008.
- [19] N. Almora-Barrios, G. Novell-Leruth, P. Whiting, L. M. Liz-Marzán and N. López, "Theoretical Description of the Role of Halides, Silver, and Surfactants on the Structure of Gold Nanorods," *Nano Lett.*, no. 14, p. 871–875, 2014.
- [20] S. K. Meena and M. Sulpizi, "Understanding the Microscopic Origin of Gold Nanoparticle Anisotropic Growth from Molecular Dynamics Simulations," *Langmuir*, no. 29, p. 14954–14961, 2013.
- [21] C. Pierce, "The Hill Equation for Adsorption on Uniform Surfaces," *J. Phys. Chem.*, vol. 72, no. 6, pp. 1955-1959, 1968.
- [22] D. M. Schmitt, D. M. O'Dee, B. N. Cowan, J. W.-M. Birch, L. K. Mazzella, G. J. Nau and J. Horzempa, "The use of resazurin as a novel antimicrobial agent against *Francisella tularensis*," *Front. Cell. Infect. Microbiol.*, vol. 3, no. 93, 2013.